Atmos. Chem. Phys., 11, 1339–1353, 2011
www.atmos-chem-phys.net/11/1339/2011/
doi:10.5194/acp-11-1339-2011

Atmospheric Chemistry and Physics

Production, growth and properties of ultrafine atmospheric aerosol particles in an urban environment

I. Salma[1], **T. Borsós**[1], **T. Weidinger**[2], **P. Aalto**[3], **T. Hussein**[3], **M. Dal Maso**[3], **and M. Kulmala**[3]

[1]Institute of Chemistry, Eötvös University, Budapest, Hungary
[2]Department of Meteorology, Eötvös University, Budapest, Hungary
[3]Department of Physical Sciences, University of Helsinki, Finland

Received: 4 May 2010 – Published in Atmos. Chem. Phys. Discuss.: 1 June 2010
Revised: 5 February 2011 – Accepted: 10 February 2011 – Published: 15 February 2011

Abstract. Number concentrations of atmospheric aerosol particles were measured by a flow-switching type differential mobility particle sizer in an electrical mobility diameter range of 6–1000 nm in 30 channels near central Budapest with a time resolution of 10 min continuously from 3 November 2008 to 2 November 2009. Daily median number concentrations of particles varied from 3.8×10^3 to $29 \times 10^3\,cm^{-3}$ with a yearly median of $11.8 \times 10^3\,cm^{-3}$. Contribution of ultrafine particles to the total particle number ranged from 58 to 92% with a mean ratio and standard deviation of (79 ± 6)%. Typical diurnal variation of the particle number concentration was related to the major emission patterns in cities, new particle formation, sinks of particles and meteorology. Shapes of the monthly mean number size distributions were similar to each other. Overall mean for the number median mobility diameter of the Aitken and accumulation modes were 26 and 93 nm, respectively, which are substantially smaller than for rural or background environments. The Aitken and accumulation modes contributed similarly to the total particle number concentrations at the actual measurement location. New particle formation and growth unambiguously occurred on 83 days, which represent 27% of all relevant days. Hence, new particle formation and growth are not rare phenomena in Budapest. Their frequency showed an apparent seasonal variation with a minimum of 7.3% in winter and a maximum of 44% in spring. New particle formation events were linked to increased gas-phase H_2SO_4 concentrations. In the studied area, new particle formation is mainly affected by condensation sink and solar radiation. The formation process seems to be not sensitive to SO_2, which was present in a yearly median concentration of $6.7\,\mu g\,m^{-3}$. This suggests that the precursor gas was always available in excess. Formation rate of particles with a diameter of 6 nm varied between 1.65 and $12.5\,cm^{-3}\,s^{-1}$ with a mean and standard deviation of $(4.2 \pm 2.5)\,cm^{-3}\,s^{-1}$. Seasonal dependency for the formation rate could not be identified. Growth curves of nucleated particles were usually superimposed on the characteristic diurnal pattern of road traffic direct emissions. The growth rate of the nucleation mode with a median diameter of 6 nm varied from 2.0 to $13.3\,nm\,h^{-1}$ with a mean and standard deviation of $(7.7 \pm 2.4)\,nm\,h^{-1}$. There was an indicative tendency for larger growth rates in summer and for smaller values in winter. New particle formation events increased the total number concentration by a mean factor and standard deviation of 2.3 ± 1.1 relative to the concentration that occurred immediately before the event. Several indirect evidences suggest that the new particle formation events occurred at least over the whole city, and were of regional type. The results and conclusions presented are the first information of this kind for the region over one-year long time period.

1 Introduction

Ultrafine aerosol contains particles with an electrical mobility diameter smaller than 100 nm. Most of the time, their size distribution can be resolved into Aitken and accumulation modes. Residence time for the Aitken mode particles in the planetary boundary layer is relatively short. Therefore, their appearance and presence in the air in increased concentrations (which is sometimes referred to as ultrafine particle event, Woo et al., 2001; Park et al., 2008) can be directly related to their major sources. Ultrafine aerosol particles are either emitted directly from high-temperature processes or

Correspondence to: I. Salma
(salma@chem.elte.hu)

they are formed in the air as secondary particles. Their major production types in urban environments can be identified on the basis of: the size interval in which the increased particle number concentration occurs; the correlation between the concentration of their certain size fractions and concentrations of some atmospheric pollutants (e.g., CO, NO_x or SO_2) or traffic counts; and particle growth properties (Wåhlin et al., 2001; Woo et al., 2001; Jeong et al., 2006; Watson et al., 2006; Qian et al., 2007; Park et al., 2008). They include (1) automotive road traffic emissions, for which the typical median diameter of particles is ca. 20–100 nm; (2) residential heating emissions, for which the median diameter of particles is ca. 35–100 nm for coal and fuel oil, and ca. 15–30 nm for natural gas (Shi and Harrison, 1999; Park et al., 2008); and (3) nucleation, for which the particles appearance at the lower limit of the aerosol size range of ca. 1 nm in diameter, or at the lower size limit of the measurement system. Combustion sources (production types 1 and 2) emit larger (i.e., Aitken mode) particles than those formed by nucleation (production type 3) because particles from these sources already grow inside or immediately after leaving the source due to condensation of semi-volatile substances when the exhaust or flue-gases are cooled and diluted (Shi and Harrison, 1999; Alam et al., 2003; Charron and Harrison, 2003). The size range for the road traffic emissions is consistent with the particle number size distributions for injection gasoline and diesel engines with the majority of particles in the diameter interval of 20–60 and 20–130 nm, respectively (Maricq et al., 1998; Morawska et al., 1998, 2008; Ristovski et al., 1998). Diurnal variation of the road traffic in cities has a typical time pattern with a maximum between 07:30 and 09:30 in the morning and a second broader maximum in the afternoon on workdays (e.g., Salma et al., 2004). As a consequence, similar time dependency is often observed for number concentration of particles emitted by road traffic. Particles from combustion can sometimes grow in size in urban environments mainly due to condensation of vapours formed by restricted-scale photochemical processes (Jeong et al., 2006; Park et al., 2008). This growth is mainly favoured in the afternoons. Atmospheric nucleation is thought to arise from SO_2 oxidation and probably also from the oxidation of volatile organic compounds (Jeong et al., 2004; Zhang et al., 2004b; Kulmala et al., 2007; Metzger et al., 2010; Sipilä et al., 2010; Hamed et al., 2010). It can occur as a burst or persist up to several hours (Qian et al., 2007). Organic acids were proposed to enhance new particle formation possibly through stable complex formation with sulphuric acid (Zhang et al., 2004a, b). Since the conditions for nucleation include supersaturation of some low volatility components, the freshly nucleated particles almost always grow in size. It seems likely that condensation of organic vapours contribute substantially to the growth (O'Dowd et al., 2002), and participates at least in the initial steps of the growth (Kulmala et al., 2004b). Coagulation also affects the growth significantly (Stolzenburg et al., 2005). In cities, particle growth is observed together with new particle formation. Primary ultrafine particles have major relevance for the air quality and emission source apportionment. Nucleation, however, usually happens on larger spatial scales than the other two production types, and it influences the global particle budget significantly as one of the basic atmospheric aerosol processes (Kulmala et al., 2004a).

Atmospheric ultrafine aerosol particles can grow into the size range of cloud condensation or ice nuclei. They influence the indirect climate effects of atmospheric aerosol, and water cycling (Andreae and Rosenfeld, 2008 and references therein). The uncertainty of their climate impacts belong to the largest single contributions in the atmospheric radiative forcing calculations. Ultrafine aerosol particles are present in large numbers in polluted urban, workplace or indoor air, and they represent specific health risks relative to coarse or fine particles of the same or similar chemical composition. They can enter directly into the bloodstream from the lungs, and can be deposited in various sensitive organs in the body such as the heart or central nervous system (Oberdörster et al., 2005 and references therein). With the advancement and applications of nano-science and – technology, the relevance of the topic is expected to increase further because they or their products potentially emit ultrafine particles into the air.

Time evolution of number size distributions makes it feasible to study new particle formation and particle growth. However, the available instruments do not allow the direct measurement of nucleated particles at present but they are limited to a certain size. The detection limit has been recently moved to diameters being nowadays smaller than 1.5 nm (Mirme et al., 2010; Sipilä et al., 2010). This means that the initial particles, which mass diameters are considered to be around 1 nm (Kulmala et al., 2000, 2005b) and electrical mobility diameters around 1.5 nm, will already be observed if proper instruments are available. However, the measurements typically yield formation rates (J_d, at a measurable diameter $d > 1.5$ nm) instead of nucleation rates ($J_{1.5}$), and $J_d < J_{1.5}$ under steady state conditions. The relationship between nucleation and formation rates is influenced by the competition between condensational growth (which also depends on the condensing vapour concentrations) and coagulation scavenging, and it strongly depends on the size distribution of the pre-existing aerosol particles. Evaluation of the experimental data from atmospheric measurements is disturbed by large associated uncertainties of the input data, sensitivity of the theoretical model to the uncertainties, and by some unknown variables. In addition, it was revealed that the nucleation process is tied to the existence of sub-3 nm pool of neutral and charged clusters which exists almost all the time (Kulmala et al., 2005b, 2007; Sipilä et al., 2008; Mirme et al., 2010), and which further obscures the description. The exact growth behaviour for the initial phase is unknown. Therefore, formation rates are derived and interpreted in the present paper rather than nucleation rates.

New aerosol particle formation events and particle growth were observed around the world in a variety of geographic

locations and ambient conditions in both the boundary layer and free troposphere including remote (Arctic, Antarctic or Alpine) locations, coastal environments, boreal forests, rural, agricultural and urban sites, polluted cities, volcanic emissions and exhaust plumes. The observations were reviewed by Kulmala et al. (2004a), Holmes (2007), and Kulmala and Kerminen (2008). It was concluded that long-term continuous measurements in all types of environment are desirable for better understanding and quantifying the mechanism, the extent of production, and role of ultrafine particles in more detail. Considering this, number size distributions of atmospheric aerosol particles were determined in an electrical mobility diameter range of 6–1000 nm near central Budapest continuously for one year, as a follow up of our research on urban aerosol (e.g., Salma et al., 2005, 2006, 2007; Maenhaut et al., 2005) and with the primary purpose of studying new particle formation in an urban environment. The main objectives of this paper are: to report average atmospheric particle number concentration and its diurnal variation for several size fractions; to present individual and mean particle number size distributions; to discuss the occurrence of new particle formation events; to derive and evaluate particle formation and growth rates; to study the seasonal dependency of properties mentioned; to assess the major controlling variables for new particle formation; to estimate the spatial scale of the new particle formation events. These results represent the first information of this kind for the region, i.e., for Hungary or for the Carpathian basin over a one-year long time period.

Fig. 1. Map of Budapest showing the central part of the city (indicated by red line) and the measurement location (marked by red dot) at the campus of the Eötvös University downwind from the central urban part, on the bank of the river Danube.

2 Experimental

2.1 Measurements

The measurements were carried out in the Lágymányos campus of the Eötvös University in Budapest (47°28′29″ N, 19°03′43″ E, 115 m above the m.s.l.). The location is near the central part of the city in downwind direction. The major pollution sources include automotive road traffic, residential and commercial heating, biomass burning and biogenic emissions within the agglomeration. Long-range transport of some pollutants also plays a considerable role (Salma et al. 2001, 2004; Salma and Maenhaut, 2006). Diesel-powered vehicles shared 20% of the national passenger car fleet in 2009; the mean lifetime of passenger cars registered in Budapest was 9.4 yr (OKJ, 2010). The measurements were performed in a distance of about 80 m from the bank of the river Danube. The site is influenced by a wind channel which is formed above the river. The prevailing wind direction in Budapest is NW. It brings clean air into the central part, dilutes the polluted air there, and leaves almost unrestrictedly in the S-SE direction. The location is displayed in Fig. 1. The map also reveals the advantageous relationship between the prevailing wind direction and orientation of the natural topological forms. The measurements were performed continuously from 3 November 2008 to 2 November 2009, thus for one year. An overview on days with available and missing data is shown in Table 1. No data are missing at all for 90% of the days. This means that the acquired data sets are representative.

The measurement system consisted of a flow-switching type differential mobility particle sizer (DMPS) and a meteorological station. The sampling line for the DMPS was made of Cu tubing with an internal diameter of 4 mm and length of approximately 2 m. There was no upper size cut-off inlet applied to the sampling line, and a weather shield was only adopted. The main parts of the DMPS include a ^{241}Am neutralizer, a Nafion semi-permeable membrane drier, a 28-cm long Hauke-type differential mobility analyser and a butanol-based condensation particle counter (CPC, model 3775, TSI, USA). The DMPS operates at two sets of flows. In the first (high flow) mode, the sample air and sheath air flows are 2 and 20 l min^{-1}, respectively, while in the second (low flow) mode, they are 0.3 and 3 l min^{-1}, respectively (Aalto et al., 2001). The DMPS records particle

number concentrations for a unity logarithmic electrical mobility diameter ($dN/d\log d$, where N is the particle number concentration) from 6 to 1000 nm in 30 channels. Of them, 20 channels were recorded during the high flow, and 10 channels were acquired during the low flow. This means that particles with a diameter from 6 to 200 nm were measured during the high flow mode, and particles with a diameter from 200 to 1000 nm were measured during the low flow mode. Measuring the whole size range of interest takes approximately 10 min, which was set as the compromise between the time resolution and particle counting statistics. This choice yielded ca. 138 spectra a day. The size separation in the DMA was tested and calibrated by using spherical polystyrene latex particles with a diameter of 400 nm. The performance of the DMPS to measure the total number of particles accurately was tested with another CPC (model 3786, TSI, USA) with a lower measurement limit of 2.5 nm. It was operated in parallel with the DMPS system on a day when aged aerosol was dominating. The DMPS-to-CPC3786 concentration ratio was 0.93 ± 0.14, and a correlation coefficient of $R = 0.933$ ($p < 2 \times 10^{-4}$) was obtained. These values indicate a satisfactory agreement between the two instruments (Morawska et al., 2008). Operational parameters (flows and high voltage values) of the DMPS were checked and calibrated at least once in two weeks. Nevertheless, measured concentration data in the very first channel occasionally contained significant amount of instrumental noise. Such situation is also detectable in Fig. 5. In these few cases, the first individual data in the size spectrum was removed from the data set. It has to be also mentioned that the DMPS operates in a dried sample flow (with typical relative humidities between 10 and 25%) and, hence, the results obtained refer to the dry state of particles.

Basic meteorological data with a time resolution of 10 min were obtained from the Urban Climatological Station of the Hungarian Meteorological Service operated in the university campus. Mean air temperature, ambient relative humidity, solar radiation and wind speed for the period studied were 11.5 °C, 66%, 144 W m^{-2} and 2.9 m s^{-1}, respectively. Daily mean SO_2 concentration data for central Budapest were obtained from municipal authorities. The mean concentration varied from 3.3 to 30 µg m^{-3} for the time interval considered with a yearly median of 6.7 µg m^{-3} (see also Table 2).

2.2 Data treatment

The measured data were mathematically inverted on-line after each measurement cycle. The inverted individual data were used for calculating particle number concentrations in the diameter ranges from 6 to 1000 nm (N_{6-1000}), from 6 to 100 nm (N_{6-100}) and from 100 to 1000 nm ($N_{100-1000}$) with a time resolution of ca. 10 min. The former two size fractions represent the total number of aerosol particles and the ultrafine particles, respectively (see Sect. 3.3), while the latter size fraction can be associated with a larger region. Daily and yearly average concentrations were calculated for the size fractions, and diurnal variation of concentrations averaged by the time of day separately for days with new particle formation and days with no new particle formation were also derived. The inverted individual concentration data were also averaged separately for every month to derive monthly mean number size distributions. In a few cases, daily mean number size distributions were also derived. The distributions were fitted by lognormal functions using the DoFit algorithm (Hussein et al., 2005) to obtain the modal concentrations, number median mobility diameters (NMMDs) and geometric standard deviations (GSDs) for the modes identified. The relative uncertainty of the fitted parameters usually remained below 10–15%. The uncertainties, in particular for modal concentration, can be significantly increased under some limiting circumstances (as in Fig. 4b). Therefore, number concentrations in the diameter range from 6 to 25 nm (N_{6-25}) were preferably used in the further calculations instead of nucleation mode concentrations.

The inverted individual concentrations were utilised to generate contour plots showing jointly the time variation in particle diameter and normalised particle number concentration. The plots were classified on a day-to-day basis. The time interval considered is justified by the fact that all new particle formation events appeared in the daytime and were virtually finished by the evening (see Sect. 3.4). The classification was accomplished via an algorithm similar to that proposed earlier (Dal Maso et al., 2005). The relevant days were classified visually by two experts into the following groups: new particle formation event class 1, new particle formation event class 2, no new particle formation event, and event with undefined feature. Each day was assigned only to one of the classes. The main purposes of this classification were (1) to separate the days with evident new particle formation event, (2) to select the days with unambiguously no new particle formation, and (3) to create a statistical overview on them. To achieve goal 1, new particle formation should be clearly distinguished from the direct emissions of local combustion sources and restricted-scale photochemical growth. Therefore, the classification scheme involves the criteria for both the appearance of a new mode at the detection limit of the instrument, and its remarkable growth subsequently. However, we are aware that there are no discrete boundaries between the groups. The space available for the formation process can, for example, affect the contour plots. Increase in the nucleation mode NMMD is not expected to be observed if the spatial extension of the nucleation is restricted to a point or line, and if the new particles are transported by horizontal advection to a fixed measurement site that is in a close distance from the new particle formation area (Kulmala et al., 2004a). The algorithm works well for relatively large open spaces such as our measurement site. Fluctuations caused by the turbulent nature of the atmosphere, and limitations inherent to every spatially fixed single measurement setups can also hinder the classification and evaluation.

New particle formation events of class 1 represented processes without disruptions and, therefore, were further analysed. Each individual size distribution on these days were fitted using the DoFit algorithm (Hussein et al., 2005), and the modal parameters for the nucleation, Aitken and accumulation modes were derived. A subset of 31 new particle formation events (called class 1A) could be separated from the total number of 42 class 1 events for which the nucleation mode was so well developed in time that the evolution of its parameters made it feasible to calculate particle formation and growth rates. Time evolution of an aerosol population is described by the general dynamic equation (Seinfeld and Pandis, 1998) which can be approximated by (Kulmala et al., 2001; Dal Maso et al., 2002):

$$J_d = \frac{\mathrm{d}N_{\mathrm{nuc}}}{\mathrm{d}t} + F_{\mathrm{coag}} + F_{\mathrm{growth}}\,, \tag{1}$$

where J_d is the flux of particles into the observable size range at diameter d, N_{nuc} is the number concentration of nucleated particles, F_{coag} expresses the loss of particles due to coagulation, F_{growth} is the flux of particles out of the size range due to growth, and t is time. The effects of horizontal advection and mixing from above are not taken into consideration in this approach. For regional new particle formation events, horizontal inhomogeneity is thought to be negligible. For our measurement system: $J_d = J_6$. The size range for the nucleated particles was chosen to be from 6 to 25 nm, thus $N_{\mathrm{nuc}} \approx N_{6-25}$. In this way, F_{growth} can be neglected since particles rarely grow out from this range before the formation ends (Dal Maso et al., 2005). It was presumed that the intensity of the nucleation source is constant for a certain time period, and hence $\mathrm{d}N_{6-25}/\mathrm{d}t$ was determined as the slope of the function N_{6-25} versus time within a period that could be approximated by a linear fit. The computation of the coagulation loss term was adopted from the procedure of Dal Maso et al. (2005). In short, the coagulation rate was expressed as:

$$F_{\mathrm{coag}} = \mathrm{CoagS}_{\mathrm{nuc}}\, N_{\mathrm{nuc}} \approx \mathrm{CoagS}_{\mathrm{NMMD}}\, N_{6-25}\,, \tag{2}$$

where $\mathrm{CoagS}_{\mathrm{nuc}}$ is the coagulation scavenging efficiency of particles in the nucleation mode. In Eq. (2), it was approximated by the coagulation scavenging efficiency for the NMMD of the nucleation mode. The mean value of F_{coag} over the observed linear formation period was derived, and it was adopted in the calculation of formation rates. This procedure represents an effective method that handles fluctuating data well.

Growth rate is the rate at which a characteristic diameter of an aerosol particle, population or size mode grows. Median diameter for the nucleation mode was considered to be the characteristic diameter of the nucleated aerosol population. Growth rates also depend on time. To estimate its value at the lower measurement limit of 6 nm, a linear line was fitted to the first several NMMD data in its time evolution plot, and the growth rate value was derived from the slope of the fitted line.

Aerosol condensation sink (CS) is a key property that expresses the ability of aerosol particles to remove condensable vapours from the atmosphere. Hence, it influences the particle growth, and strongly depends on the size distribution of pre-existing aerosol particles. Condensation sink was calculated using the procedure described in Dal Maso et al. (2005) as:

$$\mathrm{CS} = 2\pi D \sum_i \beta_M(d_{p,i})\, d_{p,i}\, N_i\,, \tag{3}$$

where D is the diffusion coefficient of the condensing vapour, $d_{p,i}$ and N_i are the diameter and number concentration of particles, respectively in size bin i. The transition correction factor for the mass flux $\beta_{\mathrm{M}}(d_{p,i})$ accounts for the differences in the condensation flux at small and large particle sizes, and it was calculated by using the Fuchs-Stutugin expression with a mass accommodation coefficient assumed to be unity. The equilibrium vapour pressure of the condensing species was assumed to be negligible at the surface of the particles (Kulmala et al., 2001), so similar of sulphuric acid. No information was available on the hygroscopic properties of aerosol particles in Budapest, and, therefore, the calculations of CS were based on dry diameters, and the extent of the CS underestimation was assessed. Condensation sink was obtained for each individual size distribution. Condensation sink can be also regarded as the coagulation sink of vapour-molecule-sized particles. Hence, CS was further utilized to estimate the coagulation sink (CoagS_{dp}) for the smallest (usually recently formed) particles by the relationship (Lehtinen et al., 2007):

$$\mathrm{CoagS}_{d_p} = \left(\frac{0.71}{d_p}\right)^{-m} \mathrm{CS}, \tag{4}$$

where m is an empirical factor that generally can be assumed to be constant of ca. $m \approx 1.7$ (Dal Maso et al., 2008). Collisions with pre-existing particles are the main sink for the smallest particles. Atmospheric residence time of condensing vapour and freshly formed particles were estimated from the inverse of CS and CoagS_{dp}, respectively.

Gas-phase H_2SO_4 plays a central role in atmospheric new particle formation, cluster activation and particle growth (see Sect. 1). Unfortunately, H_2SO_4 vapour was not measured in Budapest during the time period considered. Instead, a simple but reasonable proxy containing both source and sink terms for H_2SO_4 was calculated (Petäjä et al., 2009). In the lower troposphere, H_2SO_4 is produced in the gas phase mainly by the reaction of SO_2 with OH radical. The concentration of OH radical depends primarily on the intensity of solar radiation. The main sink for gas-phase H_2SO_4 is collisions with aerosol particles. Concentration of H_2SO_4 vapour ($[H_2SO_4]$) can be formally related to a proxy that is obtained from SO_2 concentration ($[SO_2]$), solar radiation (Rad) and CS as:

$$[\mathrm{H_2SO_4}] \propto \frac{[\mathrm{SO_2}]\cdot \mathrm{Rad}}{\mathrm{CS}}. \tag{5}$$

Solar radiation and SO_2 concentration were measured by pyranometer and UV fluorescence analyser, respectively. For SO_2, only daily means were available, and, therefore, the calculations are based on the daily means.

3 Results and discussion

3.1 Average atmospheric concentrations

Daily median N_{6-1000} concentrations varied from 3.8×10^3 (8 March) to 29×10^3 cm^{-3} (9 January) with a yearly median of 11.8×10^3 cm^{-3}. The data set exhibited logarithmically normal distribution, which was proven by cumulative log-probability graph (Hinds, 1999). The concentration distribution was characterized by a GSD of 1.43. It is noted for comparison, that the daily median PM_{10}-fraction aerosol mass concentration (measured by beta-gauge) for the same time period was also log-normally distributed with a GSD and median of 1.78 and 28 µg m^{-3}, respectively. Comparison of the GSDs implies that there was not much fluctuation in the production and removal of particles in terms of numbers on a daily basis (see also Fig. 2). Reasons for this relatively small time variation are given in Sect. 3.3. The number concentrations are comparable to, but smaller than, the typical values of $(15–23) \times 10^3$ cm^{-3} reported for other urban environments (Väkevä et al., 2000; Woo et al., 2001; Jeong et al., 2006; Watson et al., 2006; Qian et al., 2007; Park et al., 2008). Time variation of the daily median concentration for the whole year is shown in Fig. 2. It is seen that the concentration shows no evident seasonal tendency, similarly to some criteria air pollutants such as SO_2, NO and NO_x. This differs from some other cities, where the largest monthly concentration was observed in February, and the smallest monthly concentration in July (Jeong et al., 2006). The two largest values for 9 and 10 January stand out from the other data. They relate to a period when a smog alert was announced for Budapest (11 and 12 January 2009). Daily median N_{6-100} (ultrafine particle) concentration ranged from 2.7×10^3 (8 March) to 20×10^3 cm^{-3} (9 January) with a yearly median of 9.3×10^3 cm^{-3}. Its time variation is also shown in Fig. 2.

Strong association between N_{6-100} and N_{6-1000} is evident from their correlation coefficient of 0.972 ($p < 10^{-4}$). Contribution of ultrafine particles to the total particle number, calculated as the N_{6-100}/N_{6-1000} concentration ratio, varied from 58% (29 December) to 92% (20 July). Daily median concentration ratios did not show marked seasonal tendency. The individual ratios were averaged for the whole year, separately for the days with new particle formation, and for the days without new particle formation. Mean ratios and standard deviations of (79 ± 6)%, (82 ± 5)% and (78 ± 6)% were obtained for the data sets listed, respectively. This is linked to the fact that large primary emissions and new particle formation events occur alternatively in Budapest, and the combination of these two effects maintains a more or less constant

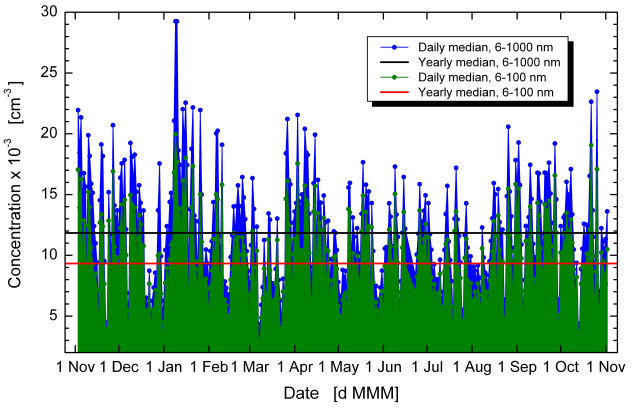

Fig. 2. Median particle number concentrations in the diameter ranges from 6 to 1000 nm and from 6 to 100 nm near central Budapest from 3 November 2008 to 2 November 2009.

ultrafine contribution (see also Sects. 3.2 and 3.3). The yearly mean ratio is comparable to, but somewhat smaller than, the range of 88–94% reported for some other cities (Jeong et al., 2006). For the most polluted two days of 9 and 10 January, the ratios were 68 and 60%, respectively, which are at the lower end of the interval observed. Nevertheless, correlation between the daily median N_{6-100}/N_{6-1000} ratio and N_{6-100} or N_{6-1000} concentrations were insignificant. This implies that no linear relationship between the particle number concentration and ultrafine contribution could be established. Collectively this means that ultrafine particles make up the major fraction of the total number of particles in Budapest, and that their contribution to the total particle number is fairly constant throughout the year.

3.2 Diurnal variation of atmospheric concentrations

Diurnal variation of the mean number concentration for particles in diameter intervals of 6–100 nm and 100–1000 nm, averaged by the time of day separately for the event days and non-event days are shown in Fig. 3. It is seen that the concentration of ultrafine particles is larger than $N_{100-1000}$ by a factor of 3–4. Concentration level and time variation of ultrafine particles for the event and non-event days are very similar in the beginning. The curves show a morning peak that corresponds to morning rush hours. The maximum of the peak for the event days is considerably smaller than for the non-event days. After the maximum, the shape of the curves is different. A broad and large peak with a maximum between 13:00 and 14:00 appears for the event days. This is unambiguously explained by particle growth into and out of the measured ultrafine size interval. As expected, there is no corresponding peak for the non-event days. Interestingly, the effect of increased afternoon vehicle circulation that usually peaks between 17:00 and 18:00 in Budapest can be hardly identified on the curves. A large peak shows up in the late

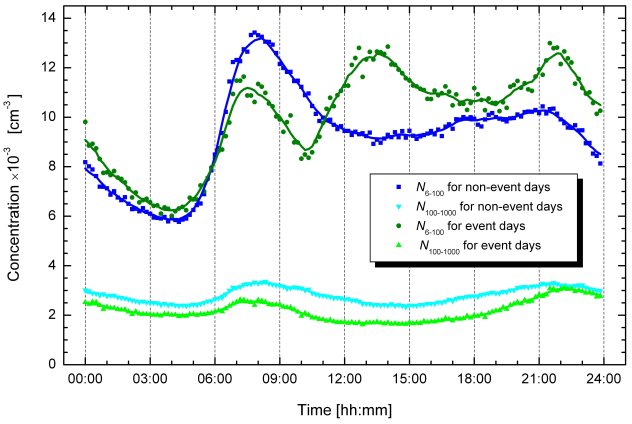

Fig. 3. Diurnal variation of the mean number concentration for particles in diameter intervals of 6–100 nm and 100–1000 nm, averaged by the time of day separately for the days with new particle formation event and without new particle formation event. The curves were obtained by 1-h smoothing and represent an eye-guide only.

evening around 21:00 and 22:00. It is much more evident for the event days than for the non-event days. Daytime variation of ultrafine particles for the non-event days was larger for summer and spring (when two well-separated morning and evening peaks occurred with a deep and broad minimum between them) than for winter and autumn (when concentration remained elevated between the two peaks). Furthermore, the second (evening) peak was shifted to earlier hours (19:00–20:00) for winter and autumn. The evening peak can be likely related to the combined effect of burning and heating activities at residences and homes, and of local meteorology. The exact interpretation of the evening peak, however, needs further investigations. Concentration of $N_{100-1000}$ for the event days is smaller than for the non-event days, which agrees with the general requirements for new particle formation (see Sect. 1). The extent of the diurnal variation of $N_{100-1000}$ concentration for both the event and non-event days is smaller than for ultrafine particles. The shape of the curves is mostly similar to each other, and both resemble the typical time-activity pattern in cities, and they are also influenced by the daily cycling of the boundary layer mixing height. The second peak occurred again in the evening. The curves become almost equal in the late evening, which is caused by the increased number concentrations due to growth processes after new particle formation events (see also Sect. 3.7).

3.3 Size distributions

The Aitken and accumulation modes were invariably present in the individual number size distributions. They merged into a broad peak which could be resolved by fitting. In general, concentration of the accumulation mode was slightly larger in the early mornings than for the Aitken mode, while the opposite was experienced in the afternoons and evenings. Averaged size distributions were fitted to obtain typical or representative modal parameters. This method, however, dismisses time resolved information and causes significant broadening of the modes. Fitting individual distributions and averaging the results was not chosen because of the huge number of size spectra measured. It is recognised that the two alternative methods do not necessarily yield completely identical results. The latter method was adopted in more detailed evaluations of some selected and shorter time periods, e.g., of days with new particle formation event. Monthly mean number size distribution for September 2009 is shown in Fig. 4a as example. Differences in the shape and relative area of the monthly mean size distributions were not substantial. Overall mean NMMDs for the Aitken and accumulation modes derived from the monthly mean distributions were (26 ± 2) nm and (93 ± 10) nm, respectively with an identical overall mean GSD of 2.1. The Aitken mode and, in particular the accumulation mode were generally shifted to smaller values than for rural or background environments, where their typical diameters are 30–60 and 150–250 nm, respectively (Raes et al., 2000; Dal Maso et al., 2005). Instrumental errors on the extent of the observed shift can be rejected. Possible explanations of the shift include several factors, e.g., the fact that dry diameters were measured in the present study, consequences of the possible overlap of multiple Aitken modes from different sources with the accumulation mode on the fitting method. The shift could be one of the particularities of central urban locations as well. The mean ratio and standard deviation of the modal concentration for the Aitken mode to that for the accumulation mode were 1.14 ± 0.11. In general, the Aitken mode was somewhat larger than the accumulation mode, which is explained by the intensity of road traffic emissions near this location. The mean size distributions also imply that the number concentration of particles with a diameter below 6 nm is negligible with respect to N_{6-100} and N_{6-1000} (except for time periods after new particle formation events which take some hours), and hence, the N_{6-100} and N_{6-1000} concentrations represent accurately the number of ultrafine aerosol particles and the total number of aerosol particles, respectively.

The nucleation mode showed up episodically at the lower detection size limit of the DMPS, and it converged progressively toward the Aitken mode for several hours. Number size distribution of particles at 10:00 local time on 8 May 2009 is shown in Fig. 4b to illustrate that the total particle concentrations are increased considerably during new particle formation events. Overall mean and standard deviation of the nucleation mode concentrations were $(10.4 \pm 2.8) \times 10^3$ cm^{-3} with a maximum daily mean of 16.1×10^3 cm^{-3}. The ratio of the mean nucleation mode concentration to the total number of particles measured for two hours just before the new particle formation event started indicates the contribution of new particle formation events to the total particle number. It ranged from 0.89 to 5.0, with a

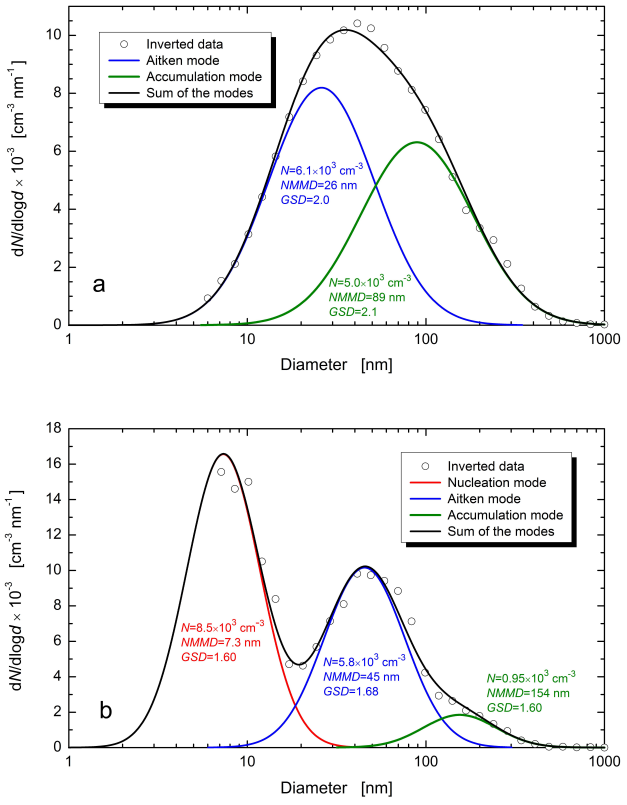

Fig. 4. Monthly mean number size distribution of atmospheric aerosol particles for September 2009 **(a)**, and number size distribution of atmospheric aerosol particles after a new particle formation event for 10:00 on 8 May 2009 **(b)**. Modal concentrations (N), number median mobility diameters (NMMD) and geometric standard deviations (GSD) for the nucleation, Aitken and accumulation modes are also shown.

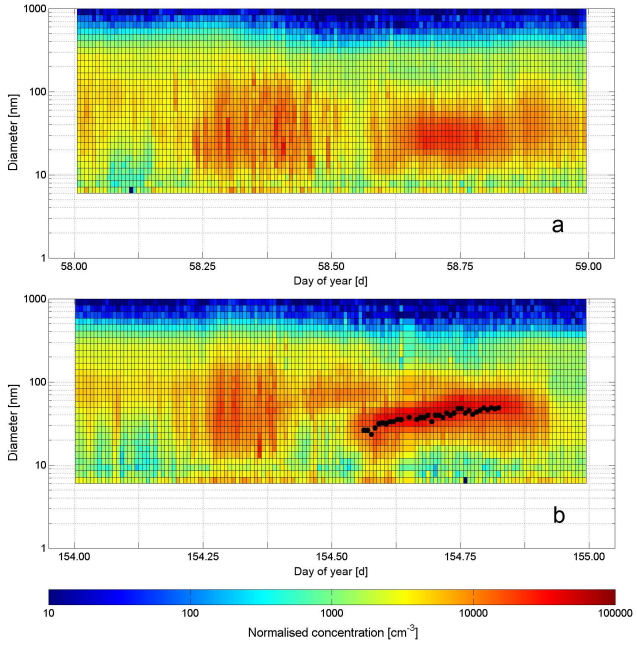

Fig. 5. Contour plots of normalised particle number concentrations showing two major automotive road traffic emission events corresponding to morning and afternoon rush hours on Friday, 27 February 2009 **(a)** and Wednesday, 3 June 2009 **(b)**. Significant growth of the primary Aitken-mode particles on **(b)** is indicated as time series of the fitted number median mobility diameter for the Aitken mode by black dots.

mean and standard deviation of 2.3 ± 1.1. Ratios below unity correspond to situations when the number concentration of particles from traffic emissions decreased suddenly just before the new particle formation event started due to mixing of air parcels, and due to changes in traffic circulation. New particle formation events occur when the number concentration levels are relatively low, and they increase the concentrations considerably. Combination of these two effects smoothes the variability in the daily average concentrations mentioned in Sect. 3.1. The nucleation mode could not be identified in the monthly mean number size distributions because of its shifting position and relatively large concentrations for the Aitken and accumulation modes. Evaluations in the further sections are based on fitted individual size distributions.

3.4 Time evolution of size distributions

Typical contour plots for traffic emissions and/or new particle formation events on four separate days are shown in Figs. 5a, 5b, 6a and 6b as examples. It is seen in Fig. 5a that the number concentration of aerosol particles in the diameter range of 25–100 nm started to increase substantially around 06:00, due mainly to high intensity of road traffic (Salma et al., 2004). The concentration peaked around 07:30 and then it decreased monotonically due to decreasing traffic intensity, and as different air parcels – such as those containing hotter exhaust gases and cooler ambient air (possibly from the boundary layer of the previous day – were mixed. The concentration decreased substantially by 11:00 when the morning rush hours were over. Increased N_{25-100} concentrations were observed again from about 14:30 for the afternoon rush hours until late evening. The high evening levels lasted for longer time which can be related to several factors. It is thought that local meteorology plays an important role among them. More stable boundary layer mixing height in the late afternoon and evening, larger mixing in the afternoon and early evening, and smaller wind speed during late afternoons can all contribute. In addition, residential burning processes produce particles in this time period. These (Aitken-mode) particles occasionally exhibited demonstrable growth on sunny afternoons. Such situation is shown in Fig. 5b. Numbers of these days for each season and whole year are indicated in Table 1. Its frequency relative to the days without obvious new particle formation showed a maximum of 46% in summer when the photo-chemical activity

is usually large. Mean concentration level of ozone – and expectedly, concentrations of other photo-chemically derived compounds including condensing organic vapours – were higher during these days than the yearly average. Furthermore, the weather was typically calm, the wind speed was usually low and wind direction was stable on these days. This type of modal growth is, therefore, interpreted as condensation of vapours formed by restricted-scale photo-chemical reactions. Typical growth rates observed for the Aitken mode are close to the growth rates derived for the nucleation mode (see Sect. 3.6). However, it is important to distinguish these growth events from the new particle formation and consecutive growth because the former processes involve already existing particles. Similar phenomena were interpreted earlier as morning particle formation event or local SO_2-related particle formation event (Jeong et al., 2006). At the same time, other relevant features of new particle formation events – e.g., particle growth right from the detection limit (which was at 10 nm) that occurs in the absolute majority of cases in cities (Qian et al., 2007) – were not identified in these two formation types. Our interpretation of direct emissions can include these earlier results as well. In any case, the issue emphasizes that the diameter interval $<$10 nm is crucial for making distinction between emission and formation events, and it should be definitely covered by contemporary measurement systems.

Figure 6a demonstrates that both road traffic emissions and new particle formation can contribute substantially to atmospheric number concentrations on the very same day. At present, we only have indirect evidences that new particle formation in Budapest is strongly influenced by atmospheric processes related to urban climate (heat island), which can be invoked as working hypothesis for the time being. It is seen in Fig. 6a that N_{25-100} concentration dropped around 09:30 likely due to decreased road traffic intensity and as a result of the mixing of the air parcels mentioned above. New particle formation was initiated. The nucleated particles grew in size and reached the detection size limit of the instrument at 10:34. Their growth was traced from this instant for several hours. The wide onset of the growth curve indicates a sustained new particle formation event for a longer time (up to 6 h). By the beginning of the afternoon rush hours, at around 14:30, the nucleation mode had grown to a mode characterised by an NMMD of approximately 18 nm. It overlapped with the distribution of particles from traffic emissions that emerged again due to the increased road traffic. Their superposition led to a modest but sudden shift in the fitted nucleation mode NMMD at 14:34, which is an artefact of the fitting procedure. It was caused by unresolved multiplets of two peaks. The secondary (nucleated) particles were mixed with the primary particles before they reached their ultimate size. This type of the contour plots represents the ordinary time evolution of the size distributions for the event days. Only a few growth processes occurred without disturbances from direct sources. One of them is shown in Fig. 6b. A cold weather front passed the city in the afternoon and evening on Friday, 7 November, and it removed the air pollutants from the agglomeration, creating clean atmospheric conditions. Lower traffic densities and emissions on the next day (Saturday) also influenced the actual time development advantageously. The narrow onset of the growth curve suggests that the new particle formation event occurred in a short time interval as a burst. The nucleated and grown particles were detected from 08:32. Evolution of the NMMD for the nucleation mode was well developed and it reached its ultimate value at approximately 60 nm. The contribution of the traffic emissions in the morning and afternoon was weak on Saturday though emissions are still visible on the contour plot.

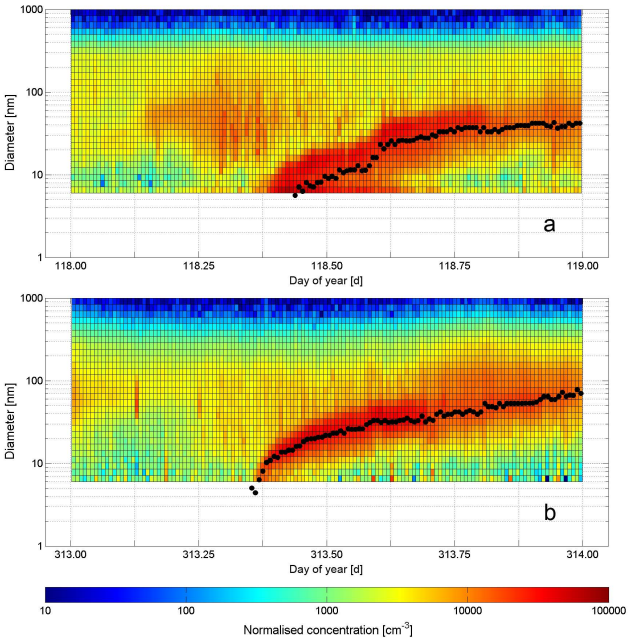

Fig. 6. Contour plots of normalised particle number concentrations measured on Tuesday, 28 April 2009 displaying road traffic emission events and a new particle formation in the midday together with a consecutive particle growth **(a)**, and on Saturday, 8 November 2008 showing a new particle formation and consecutive particle growth **(b)**. Time series of the fitted number median mobility diameters for the nucleation mode are indicated by black dots on both panels.

There was one more type of contour plots identified. It shows a steady-state concentration for all particle diameters over the whole day either at low or high concentration levels.

3.5 New particle formation event statistics

Basic statistics on days considered, days with missing data, days with evident new particle formation event, days with unambiguously no new particle formation event, and days with undefined feature for the four seasons and whole year

Table 1. Total number of days considered, number of days when measurement data were missing for more than 4 h, days with undefined new particle formation feature, days with evident new particle formation event, and days obviously without new particle formation event for the four seasons and whole year near central Budapest from 3 November 2008 to 2 November 2009. Number of days for the major subclasses of new particle formation, i.e., Classes 1A, 1B and 2; and number of days with obviously no new particle formation but with substantial growth of the Aitken mode are also indicated.

	Winter	Spring	Summer	Autumn	Year
Days	90	92	92	91	365
Days with missing data	3	2	10	4	19
Undefined days	5	12	7	10	34
Days with new particle formation	6	34	21	22	83
Days with Class 1A event	1	11	6	13	31
Days with Class 1B event	1	5	4	1	11
Days with Class 2 event	4	18	11	18	41
Days with no new particle formation	76	44	54	55	229
Days with Aitken-mode growth	24	9	25	17	75

are shown in Table 1. Number of days for the major subclasses of new particle formation, i.e., classes 1A, 1B and 2; and number of days with obviously no new particle formation but substantial growth of the Aitken mode are also indicated in the table. It is seen that new particle formation events are not rare in Budapest. They occurred on 83 days, which represent 27% of all relevant days. New particle formation frequency exhibited a remarkable seasonal variation with a minimum of 7.3% in winter and a maximum of 44% in spring. In summer and autumn, the frequencies were similar to each other with a value of 28–29%. The frequencies of the non-event days complement these values to unity. The numbers of days that could not be classified into the two main categories were 5, 12, 7 and 10 for winter, spring, summer and autumn, respectively. Their undefined feature could be caused by disturbances from local pollution sources and, more importantly, by limitations of all measurements at a fixed site which can be exposed to spatially inhomogeneous air masses causing repeatedly or completely discontinued modal growth. These days were removed from the statistics but their maximal contribution is smaller than the seasonal variation in the frequency. Therefore, they do not alter the tendency observed. The new particle formation frequencies are similar to those at urban St. Louis, USA with a minimum of 8% in winter and a maximum of 36% in April-September (Qian et al., 2007). Figure 7 shows monthly mean new particle formation frequencies throughout the year. It is seen that the largest frequency occurred in April, and a local maximum appeared in September. The distribution has no clear time dependency over the rest of the year. The largest new particle formation activity was observed during summer (July) in urban St. Louis, USA (Qian et al., 2007), in spring (April) in the Hyytiälä forest, Finland (Dal Maso et al., 2005) and at Rochester, NY (Jeong et al., 2006), and in winter (January) and spring (April) in the Hohenpeissenberg mountain, Germany (Birmili et al., 2003). Annual frequency and seasonal variation of new particle formation are known to be related to local features, e.g., to solar radiation, air temperature, relative humidity, biogenic emissions, local wind speed, boundary layer height, and concentration and size distribution of atmospheric aerosol particles (Väkevä et al., 2000; Kulmala et al., 2004a; Kiendler-Scharr et al., 2009). The new particle formation activity may be also associated with some limiting or triggering atmospheric processes in the actual region. The reasons for new particle formation events in Budapest, relationships between their properties, pollutant gases and meteorological variables are to be dealt with in a separate paper.

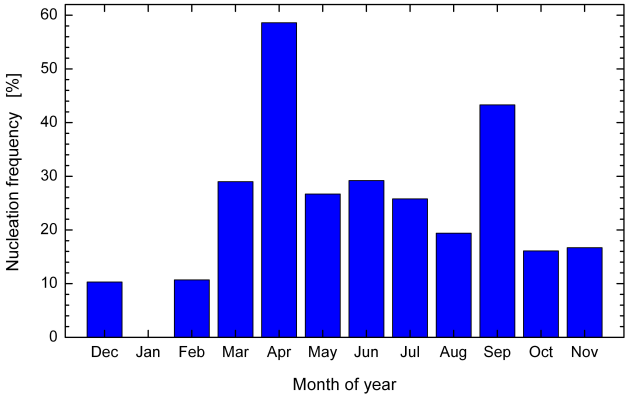

Fig. 7. Monthly mean new particle formation frequency in Budapest from 3 November 2008 to 2 November 2009.

3.6 Formation and growth rates

Formation rates of particles with a diameter of 6 nm are shown in Fig. 8a. They vary between 1.65 and 12.5 $cm^{-3}\,s^{-1}$ with a mean and standard deviation of $(4.2 \pm 2.5)\,cm^{-3}\,s^{-1}$. Coagulation losses represented approximately 20–130% of

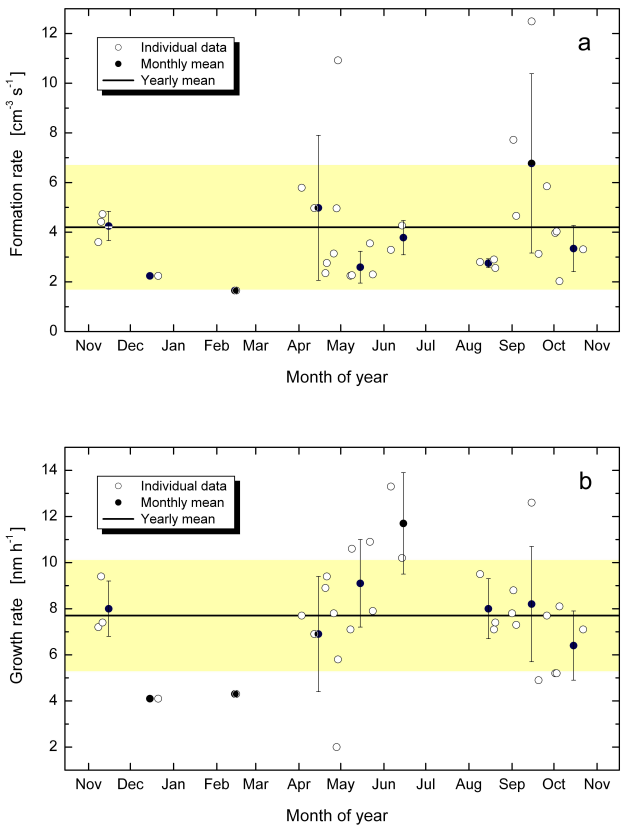

Fig. 8. Formation rates of aerosol particles with a diameter of 6 nm **(a)**, and growth rate of the nucleation mode with a median diameter of 6 nm **(b)** in Budapest from 3 November 2008 to 2 November 2009. Error bars represent standard deviations. Standard deviation of the yearly mean is indicated by yellow area.

the particle flux dN_{6-25}/dt with a mean of 77%. This indicates the importance of coagulation for nucleated particles in cities since the directly observable particle flux was on average ca. 60% of the real formation rate. The rate values derived are comparable to other urban data and larger than the values for background environments (Kulmala et al., 2004a and references therein; Yli-Juuti et al., 2009), though they were often reported for different diameters of 3 or 10 nm. Monthly mean formation rates are also included in Fig. 8a. Seasonal dependency could not be identified on the basis of the individual data or of the mean values because of their spread and limited number.

Individual growth rate values and monthly means are shown in Fig. 8b. The growth rates range from 2.0 to 13.3 nm h^{-1} with a mean and standard deviation of (7.7 ± 2.4) nm h^{-1}. They essentially fit into the ranges of 3–11 nm h^{-1} (Alam et al., 2003), 2–6 nm h^{-1} (Kulmala et al., 2004a), 1.1–16.0 nm h^{-1} (Kulmala et al., 2005a), 3–22 nm h^{-1} (Stolzenburg et al., 2005), 5–13 nm h^{-1} (Jeong et al., 2006), (5.9 ± 4.7) nm h^{-1} (Qian et al., 2007), and 2–5 nm h^{-1} (Park el al., 2008) reported for other urban environments. It is realised that growth rates for various locations were not given for exactly the same particle diameters. There is a tendency for larger growth rates in summer, and for smaller values in winter in our data sets but the number of data available (in particular for winter) does not make it feasible to quantify the tendency. This indicative dependency becomes more evident when the monthly mean growth rates are considered. It is consistent with the tendency observed at another urban location (Qian et al., 2007) and other background sites (Kulmala et al., 2004a). The larger summertime growth rates probably reflect the larger concentrations of condensing vapours due to enhanced photochemical activity, and also to increased biogenic organic precursor emissions. This is consistent with observations at other locations (Birmili et al., 2003; Dal Maso et al., 2005; Qian et al., 2007).

3.7 Condensation sink and gas-phase sulphuric acid proxy

Individual condensation sink ranged from 1.2×10^{-3} s^{-1} to 101×10^{-3} s^{-1} with a mean and standard deviation of $(16 \pm 10) \times 10^{-3}$ s^{-1}. As expected, the values are larger than for rural or background environments (Dal Maso et al., 2005), and they are comparable to the range of (3.2–150) $\times 10^{-3}$ s^{-1} for some European cities (Kulmala et al., 2005a). It has to be noted that dry particle diameters were utilized in the evaluation, which do not necessarily represent ambient wet conditions well. Unfortunately, no information is available at present on the hygroscopic properties of aerosol particles in Budapest. Hence, the presented CS values can be regarded as lower estimates for real condensation sinks. Calculation in which use was made of the hygroscopic growth factors of $(NH_4)_2SO_4$ – which is regarded as the upper limit in realistic situations (Dal Maso et al., 2005) – yielded larger CS data by a mean factor and standard deviation of 1.24 ± 0.20. It is in agreement with the idea that the typical effect of hygroscopic growth on the CS is between 5 and 50% (Kulmala et al., 2005a).

Diurnal variation of the mean residence time for H_2SO_4 vapour and particles with a diameter of 6 nm, averaged by the time of day separately for the event days and non-event days are shown in Fig. 9. The curves exemplify the role of CS and CoagS in inhibiting new particle formation. For the non-event days, the characteristic atmospheric residence time of freshly formed particles is smaller than 40 min at its maximum, while for the event days, it is longer by 10–20 min (by ca. 50%) on average. The typical residence time for gas-phase H_2SO_4 is on the order of minutes under these conditions, thus it is much shorter than for particles. Nevertheless, the condensing vapour residence time is also longer on average by ca. 40% for the event days than for the non-event days due to a lower particle population. The longer residence time of small particles gives them time to grow to larger sizes, where they are less susceptible to coagulation scavenging. At the same time, vapour molecules have a larger chance to

Table 2. Median SO_2 concentration, solar radiation, condensation sink (CS) and gas-phase H_2SO_4 proxy averaged separately for the days with new particle formation event and without new particle formation event over the four seasons and year.

Season	Period	SO_2 [$\mu g\,m^{-3}$]	Radiation [$W\,m^{-2}$]	CS $\times 10^3$ [s^{-1}]	Proxy $\times 10^{-3}$ [$\mu g\,m^{-5}\,Ws$]
Winter	Event days	6.7	60	6.8	50
	Non-event days	8.6	37	18.7	17.8
Spring	Event days	6.1	228	12.6	93
	Non-event days	6.1	182	14.4	63
Summer	Event days	5.8	239	9.4	150
	Non-event days	5.8	244	13.7	114
Autumn	Event days	7.5	183	15.4	90
	Non-event days	7.1	78	17.5	43
Year	Event days	6.6	215	12.3	96
	Non-event days	6.8	104	15.6	47

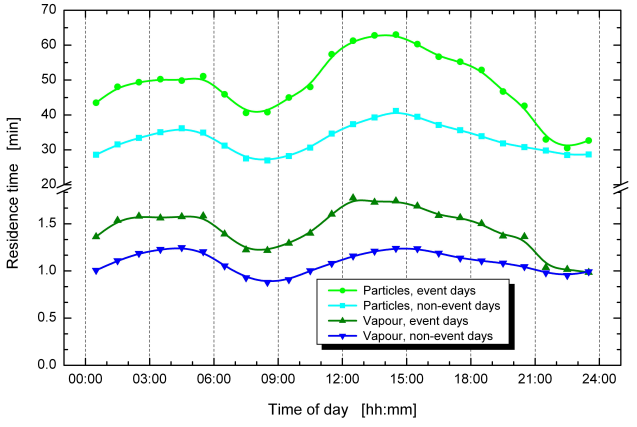

Fig. 9. Diurnal variation of the mean atmospheric residence time for H_2SO_4 vapour and particles with a diameter of 6 nm, averaged by the time of day separately for the days with new particle formation event and without new particle formation event.

condense on fresh particles – or even participate in the formation process itself – on event days, enhancing the growth rate of fresh particles. These two causes lead to the observation that lower pre-existing aerosol concentration levels are conductive to new particle formation.

This also explains the observation made in Sect. 3.2 that the non-event days exhibited larger particle concentrations in the morning, and that the initially smaller concentrations on the event days were then replenished by the formation of fresh particles (see Fig. 3). This replenishment could be also observed in the 100–1000 nm size range in the evening, when the fresh particles had had time to grow to larges sizes.

Median SO_2 concentration, solar radiation, condensation sink and gas-phase H_2SO_4 proxy averaged separately for the event days and non-event days over the four seasons and year are summarized in Table 2. It is seen that concentration of SO_2 did not change substantially for the event and non-event days. The larger value for the non-event days in winter is related to temperature inversions, some high pollution periods with SO_2 concentrations up to 30 $\mu g\,m^{-3}$, and smog alert situations (cf. Sect. 3.1). Solar radiation was larger by a factor of ca. two for the event days than for non-event days over the whole year. The difference is, however, biased by the seasonal cycle of solar radiation via the seasonal variation of new particle formation frequency. The condensation sink was smaller for the event days than for the non-event days by approximately 30% over the year. In winter, the daily average CS for the event days was smaller by 64% than for the non-event days. This can be explained by generally higher concentration level of air pollutants – including pre-existing aerosol particles – in winter due to temperature inversions that mainly occur in Budapest in winter. Combination of these three effects caused that the median H_2SO_4 proxy was larger by a factor of about two for the event days than for the non-event days over the year, and similar tendency is observed for the seasons. This clearly indicates the relationship between new particle formation and gas-phase H_2SO_4. In summer, the proxy for the event days was larger by a factor of 1.32 than for the non-event days with almost identical solar radiation for the event and non-event days. The results suggest that new particle formation in the studied area is strongly affected by condensation sink. Solar radiation also plays a role. This explains our observation that there were some series of consecutive days with new particle formation events, and the set was cut off by increased condensation sink while solar radiation and SO_2 concentration

level remained unchanged and large. No significant correlations between H_2SO_4 proxy and J_6, or between the proxy and modal growth rate at 6 nm could be identified, which was hindered by the limited number of class 1A events for which the rates were available (see Table 1).

3.8 Spatial scale of new particle formation events

Spatial scale of new particle formation is challenging with regard to sources of possible precursors or to nucleating species. Time evolution of the nucleation mode observed in Budapest (see Fig. 6a and b) is usually similar to the characteristic banana pattern observed at rural and background locations (Kulmala et al., 2004a and references therein). This shape was preserved under various horizontal advection conditions. In addition, the new particle formation events occurred around the midday and not in the early morning or late afternoon (i.e., before 08:30 or after 14:15) which is typical for large scale new particle formation events. Its horizontal scale was estimated roughly utilising the lower detection limit of the DMPS of 6 nm, the mean growth rate of $7.7\,\mathrm{nm\,h^{-1}}$ and mean wind speed of $3.7\,\mathrm{m\,s^{-1}}$ calculated for the mornings of the event days, and assuming that the air parcel containing the nucleated particles travelled with the mean wind speed. It is also realised that the particle growth rates in the initial state can be much smaller than for the nucleation mode at 6 nm. An orderly estimate of 9 km was obtained in this way, while the smallest growth rate of $2.0\,\mathrm{nm\,h^{-1}}$ resulted in a spatial scale of 33 km. The estimated extensions are comparable to the linear horizontal dimensions of the city. Some new particle formation events occurred when the local wind blew from the south or east. Horizontal extension of the nucleating air parcel is to be further expanded when considering the sustained types of new particle formation events. This suggests indirectly that the processes involved took place at least over the whole city or its larger area. The full extent of the relevant air masses within the Carpathian basin could not be assessed because of the single fixed measurement site. Further expedient studies are required to determine the spatial scale of the new particle formation more accurately. The open character of the selected location also influenced favourably the observation of meso-scale new particle formation events. It is worth noting in this respect that no new particle formation event followed by particle growth was recorded at all in Gwangju, Korea during several months in a 1-yr measurement campaign, and the missing phenomenon was explained by the limitations of the measurement location (Park et al., 2008). Selection of an appropriate urban measurement site seems to be a more sensitive issue than in rural or background environments.

4 Conclusions

Ultrafine aerosol particles dominate the total number concentrations near central Budapest by a mean contribution of 79%. They are emitted directly or generated by nucleation. The new particle formation events and subsequent particle growth identified and characterised in Budapest for the first time imply that they are definitely basic and relevant formation types in cities as well. The mean new particle formation frequency of 27% derived for a yearly interval is comparable to that for rural and background locations. Hence, new particle formation and growth are not rare phenomena in Budapest. The nucleation activity exhibits significant seasonal dependency. It is controlled by competition between the production of H_2SO_4 vapour from SO_2 and its sinks mainly by condensation. The atmospheric residence time of gas-phase H_2SO_4 is short, which indicates that its major sink is rather intensive. In the studied area, new particle formation is favoured by low pre-existing aerosol concentration level, low condensation sink, and high solar radiation. At the same time, the formation process seems to be not sensitive to SO_2, which was present in a yearly median concentration of $6.7\,\mathrm{\mu g\,m^{-3}}$. This suggests that this precursor gas is always available in excess. The processes occur in Budapest with a mean formation rate of $4.2\,\mathrm{cm^{-3}\,s^{-1}}$ and with mean growth rate of $7.7\,\mathrm{nm\,h^{-1}}$, respectively at a diameter of 6 nm. New particle formation events increase the number concentrations substantially, by a mean factor of 2.3 relative to the concentrations immediately before the event. This secondary production happens alternatively with large primary emissions from road vehicles, and their combined effect smoothes the variability in the daily average concentration. Further investigation of triggering or detailed time evolution of the phenomena are limited at present by precursor measurements with high time resolution, which were not performed in this first study in Budapest. Extended research on urban ultrafine aerosol, including new particle formation and growth in various urban microenvironments, on chemical composition and relevant physicochemical properties of ultrafine particles are undoubtedly of scientific interest with marked public-health-related implications.

Acknowledgements. Financial support of the Hungarian Scientific Research Fund (contract K61193) is appreciated.

Edited by: W. Birmili

References

Aalto, P., Hämeri, K., Becker, E., Weber, R., Salm, J., Mäkelä, J., Hoell, C., O'Dowd, C., Karlsson, H., Väkevä, M., Koponen, I. K., Buzorius, G., and Kulmala, M.: Physical characterization of aerosol particles during nucleation events, Tellus, 53B, 344–358, 2001.

Alam, A., Shi, J. P., and Harrison, R. M.: Observations of new particle formation in urban air, J. Geophys. Res., 108(D3), 4093, doi:10.1029/2001JD001417, 2003.

Andreae, M. O. and Rosenfeld, D.: Aerosol–cloud–precipitation interactions. Part 1. The nature and sources of cloud-active aerosols, Earth-Sci. Rev., 89, 13–41, 2008.

Birmili, W., Berresheim, H., Plass-Dülmer, C., Elste, T., Gilge, S., Wiedensohler, A., and Uhrner, U.: The Hohenpeissenberg aerosol formation experiment (HAFEX): a long-term study including size-resolved aerosol, H_2SO_4, OH, and monoterpenes measurements, Atmos. Chem. Phys., 3, 361–376, doi:10.5194/acp-3-361-2003, 2003.

Charron, A. and Harrison, R. M.: Primary particle formation from vehicle emissions during exhaust dilution in the roadside atmosphere, Atmos. Environ., 37, 4109–4119, 2003.

Dal Maso, M., Kulmala, M., Lehtinen, K. E. J., Mäkelä, J. M., and Aalto, P. P., and O'Dowd, C.: Condensation and coagulation sinks and formation of nucleation mode particles in coastal and boreal forest boundary layers, J. Geophys. Res., 107(19D), 8097, doi:10.1029/2001jd001053, 2002.

Dal Maso, M., Kulmala, M., Riipinen, I., Wagner, R., Hussein, T., Aalto, P. P., and Lehtinen, K. E. J.: Formation and growth of fresh atmospheric aerosols: eight years of aerosol size distribution data from SMEAR II, Hyytiälä, Finland, Boreal Environ. Res., 10, 323–336, 2005.

Dal Maso, M., Hyvärinen, A., Komppula, M., Tunved, P., Kerminen, V.-M., Lihavainen, H., Viisanen, Y., Hansson, H.-C., and Kulmala, M.: Annual and interannual variation in boreal forest aerosol particle number and volume concentration and their connection to particle formation, Tellus, B60, 495–508, doi:10.1111/j.1600-0889.2008.00366.x, 2008.

Hamed, A., Birmili, W., Joutsensaari, J., Mikkonen, S., Asmi, A., Wehner, B., Spindler, G., Jaatinen, A., Wiedensohler, A., Korhonen, H., Lehtinen, K. E. J., and Laaksonen, A.: Changes in the production rate of secondary aerosol particles in Central Europe in view of decreasing SO_2 emissions between 1996 and 2006, Atmos. Chem. Phys., 10, 1071–1091, doi:10.5194/acp-10-1071-2010, 2010.

Hinds, W. C.: Aerosol technology: properties, behavior, and measurement of airborne particles, 2nd ed., Wiley-Interscience, New York, 1999.

Holmes, N. S.: A review of particle formation events and growth in the atmosphere in the various environments and discussion of mechanistic implications, Atmos. Environ., 41, 2183–2201, 2007.

Hussein, T., Dal Maso, M., Petäjä, T., Koponen, I. K., Paatero, P., Aalto, P. P., Hämeri, K., and Kulmala, M.: Evaluation of an automatic algorithm for fitting the particle number size distributions, Boreal Env. Res., 10, 337–355, 2005.

Jeong, C.-H., Hopke, P. K., Chalupa, D., and Utell, M.: Characteristics of nucleation and growth events of ultrafine particles measured in Rochester, NY, Environ. Sci. Technol., 38, 1933–1940, 2004.

Jeong, C.-H., Evans, G. J., Hopke, P. K., Chalupa, D., and Utell, M. J.: Influence of atmospheric dispersion and new particle formation events on ambient particle number concentration in Rochester, United States, and Toronto, Canada, J. Air Waste Manage. Assoc., 56, 431–443, 2006.

Kiendler-Scharr, A., Wildt, J., Dal Maso, M., Hohaus, T., Kleist, E., Mentel, T. F., Tillmann, R., Uerlings, R., Schurr, U., and Wahner, A.: New particle formation in forests inhibited by isoprene emissions, Nature, 461, 381–384, 2009.

Kulmala, M. and Kerminen, V.-M.: On the growth of atmospheric nanoparticles, Atmos. Res., 90, 132–150, 2008.

Kulmala, M., Pirjola, L., and Mäkelä, J. M.: Stable sulphate clusters as a source of new atmospheric particles, Nature, 404, 66–69, 2000.

Kulmala, M., Dal Maso, M., Mäkelä, J. M., Pirjola, L., Väkevä, M., Aalto, P., Miikkulainen, P., Hämeri, K., and O'Dowd, C. D.: On the formation, growth and composition of nucleation mode particles, Tellus, B53, 479–490, 2001.

Kulmala, M., Vehkamäki, H., Petäjä, T., Dal Maso, M., Lauri, A., Kerminen, V.-M., Birmili, W., and McMurry, P.: Formation and growth rates of ultrafine atmospheric particles: a review of observations, J. Aerosol Sci., 35, 143–176, 2004a.

Kulmala, M., Laakso, L., Lehtinen, K. E. J., Riipinen, I., Dal Maso, M., Anttila, T., Kerminen, V.-M., Hõrrak, U., Vana, M., and Tammet, H.: Initial steps of aerosol growth, Atmos. Chem. Phys., 4, 2553–2560, doi:10.5194/acp-4-2553-2004, 2004b.

Kulmala, M., Petäjä, T., Mönkkönen, P., Koponen, I. K., Dal Maso, M., Aalto, P. P., Lehtinen, K. E. J., and Kerminen, V.-M.: On the growth of nucleation mode particles: source rates of condensable vapor in polluted and clean environments, Atmos. Chem. Phys., 5, 409–416, doi:10.5194/acp-5-409-2005, 2005a.

Kulmala, M., Lehtinen, K. E. J., Laakso, L., Mordas, G., and Hämeri, K.: On the existence of neutral atmospheric clusters, Boreal Env. Res., 10, 79–87, 2005b.

Kulmala, M., Riipinen, I., Sipilä, M., Manninen, H., Petäjä, T., Junninen, H., Dal Maso, M., Mordas, G., Mirme, A., Vana, M., Hirsikko, A., Laakso, L., Harrison, R. M., Hanson, I., Leung, C., Lehtinen, K. E. J., and Kerminen, V.-M.: Towards direct measurement of atmospheric nucleation, Science, 318, 89–92, 2007.

Lehtinen, K. E. J., Dal Maso, M., Kulmala, M., and Kerminen, V.-M.: Estimating nucleation rates from apparent particle formation rates and vice versa: Revised formulation of the Kerminen-Kulmala equation, J. Aerosol Sci. 38, 988–994, 2007.

Maenhaut, W., Raes, N., Chi, X., Cafmeyer, J., Wang, W., and Salma, I.: Chemical composition and mass closure for fine and coarse aerosols at a kerbside in Budapest, Hungary, in spring 2002, X-ray Spectrom., 34, 290–296, 2005.

Maricq, M. M., Podsiadlik, D. H., and Chase, R.: Examination of the size-resolved and transient nature of motor vehicle particle emissions, Environ. Sci. Technol., 33, 1618–1626, 1999.

Metzger, A., Verheggen, B., Dommen, J., Duplissy, J., Prevot, A. S. H., Weingartner, E., Riipinen, I., Kulmala, M., Spracklen, D. V., Carslaw, K. S., and Baltensperger, U.: Evidence for the role of organics in aerosol particle formation under atmospheric conditions, P. Natl. Acad. Sci. USA, 107, 6646–6651, 2010.

Mirme, S., Mirme, A., Minikin, A., Petzold, A., Hõrrak, U., Kerminen, V.-M., and Kulmala, M.: Atmospheric sub-3 nm particles at high altitudes, Atmos. Chem. Phys., 10, 437–451, doi:10.5194/acp-10-437-2010, 2010.

Morawska, L., Thomas, S., Bofinger, N., Wainwright, D., and Neale, D.: Comprehensive characterization of aerosols in a subtropical urban atmosphere: particle size distribution and correlation with gaseous pollutants, Atmos. Environ., 32, 2467–2478, 1998.

Morawska, L., Ristovski, Z., Jayaratne, E. R., Keogh, D. U., and Ling, X.: Ambient nano and ultrafine particles from motor vehicle emissions: Characteristics, ambient processing and implications on human exposure, Atmos. Environ., 42, 8113–8138, 2008.

Oberdörster, G., Oberdörster, E., and Oberdörster, J.: Nanotoxicology: an emerging discipline evolving from studies of ultrafine particles, Environ. Health Perspect., 113, 823–839, 2005.

O'Dowd, C., Aalto, P., Hämeri, K., Kulmala, M., and Hoffmann, T.: Atmospheric particles from organic vapours, Nature, 416, 497–498, 2002.

OKJ (National register of road vehicles, in Hungarian), Ministry of National Development, Budapest, 2010.

Park, K., Park, J. Y., Kwak, J.-H., Cho, G. N., and Kim, J.-S.: Seasonal and diurnal variations of ultrafine particle concentration in urban Gwangju, Korea: Observation of ultrafine particle events, Atmos. Environ., 42, 788–799, 2008.

Petäjä, T., Mauldin, III, R. L., Kosciuch, E., McGrath, J., Nieminen, T., Paasonen, P., Boy, M., Adamov, A., Kotiaho, T., and Kulmala, M.: Sulfuric acid and OH concentrations in a boreal forest site, Atmos. Chem. Phys., 9, 7435–7448, doi:10.5194/acp-9-7435-2009, 2009.

Qian, S., Sakurai, H., and McMurry, P. H.: Characteristics of regional nucleation events in urban East St. Louis, Atmos. Environ., 41, 4119–4127, 2007.

Raes, F., Van Dingenen, R., Vignati, E., Wilson, J., Putard, J. P., Seinfeld, J. H., and Adams, P.: Formation and cycling of aerosols in the global troposphere, Atmos. Environ., 34, 4215–4240, 2000.

Ristovski, Z., Morawska, L., Bofinger, N. D., and Hitchins, J.: Submicrometer and supermicrometer particulate emission from spark ignition vehicles, Environ. Sci. Technol., 32, 38–45,1998.

Salma, I. and Maenhaut, W.: Changes in chemical composition and mass of atmospheric aerosol pollution between 1996 and 2002 in a Central European city, Environ. Pollut., 143, 479–488, 2006.

Salma, I., Maenhaut, W., Zemplén-Papp, É., and Záray, Gy.: Comprehensive characterisation of atmospheric aerosols in Budapest: physicochemical properties of inorganic species, Atmos. Environ., 35, 4367–4378, 2001.

Salma, I., Chi, X., and Maenhaut, W.: Elemental and organic carbon in urban canyon and background environments in Budapest, Hungary, Atmos. Environ., 38, 27–36, 2004.

Salma, I., Ocskay, R., Raes, N., and Maenhaut, W.: Fine structure of mass size distributions in urban environment, Atmos. Environ., 39, 5363–5374, 2005.

Salma, I., Ocskay, R., Varga, I., and Maenhaut, W.: Surface tension of atmospheric humic-like substances in connection with relaxation, dilution, and solution pH, J. Geophys. Res., 111, D23205, doi:10.1029/2005JD007015, 2006.

Salma, I., Ocskay, R., Chi, X., and Maenhaut, W.: Sampling artefacts, concentrations and chemical composition of fine water-soluble organic carbon and humic-like substances in a continental urban atmospheric environment, Atmos. Environ., 41, 4106–4118, 2007.

Seinfeld, J. H. and Pandis, S. N.: Atmospheric chemistry and physics, From air pollution to climate change, Wiley, New York, 1998.

Shi, J. P. and Harrison, R. M.: Investigation of ultrafine particle formation during diesel exhaust dilution, Environ. Sci. Technol., 33, 3730–3736, 1999.

Sipilä, M., Lehtipalo, K., Kulmala, M., Petäjä, T., Junninen, H., Aalto, P. P., Manninen, H. E., Kyrö, E.-M., Asmi, E., Riipinen, I., Curtius, J., Krten, A., Borrmann, S., and O'Dowd, C. D.: Applicability of condensation particle counters to measure atmospheric clusters, Atmos. Chem. Phys., 8, 4049–4060, doi:10.5194/acp-8-4049-2008, 2008.

Sipilä, M., Berndt, T., Petäjä, T., Brus, T., Vanhanen, J., Stratmann, F., Patokoski, J., Mauldin III, R. L., Hyvärinen, A.-P., Lihavainen, H., and Kulmala, M.: The role of sulphuric acid in atmospheric nucleation, Science, 327, 1243–1246, 2010.

Stolzenburg, M. R., McMurry, P. H., Sakurai, H., Smith, J. N., Mauldin III, R. L., Eisele, F. L., and Clement, C. F.: Growth rates of freshly nucleated atmospheric particles in Atlanta, J. Geophys. Res., 110, D22S05, doi:10.1029/2005JD005935, 2005.

Väkevä, M., Hämeri, K., Puhakka, T., Nilsson, E., Hohti, K., and Mäkelä, J.: Effects of meteorological processes on aerosol particle size distribution in an urban background area, J. Geophys. Res., 105, 9807–9821, 2000.

Watson, J. G., Chow, J. C., Park, K., and Lowenthal, D. H.: Nanoparticle and ultrafine particle events at the Fresno supersite, J. Air Waste Manage. Assoc., 56, 417–430, 2006.

Woo, K. S., Chen, D. R., Pui, D. Y. H., and McMurry, P. H.: Measurement of Atlanta aerosol size distributions: observations of ultrafine particle events, Aerosol Sci. Technol., 34, 75–87, 2001.

Wåhlin, P., Palmgren, F., and Van Dingrnen, R.: Experimental studies of ultrafine particles in streets and the relationship to traffic, Atmos. Environ., 35, 63–69, 2001.

Yli-Juuti, T., Riipinen, I., Aalto, P. P., Nieminen, T., Maenhaut, W., Janssens, I. A., Claeys, M., Salma, I., Ocskay, R., Hoffer, A., Imre, K., and Kulmala, M.: Characteristics of new particle formation events and cluster ions at K-puszta, Hungary, Boreal Environ. Res., 14, 683–698, 2009.

Zhang, Q., Stanier, C. O., Canagaratna, M. R., Jayne, J. T., Worsnop, D. R., Pandis, S. N., and Jimenez, J. L.: Insights into the chemistry of new particle formation and growth events in Pittsburgh based on aerosol mass spectrometry, Environ. Sci. Technol., 38, 4797–4809, 2004a.

Zhang, R., Suh, I., Zhao, J., Zhang, D., Fortner, E. C., Tie, X., Molina, L. T., and Molina, M. J.: Atmospheric new particle formation enhanced by organic acids, Science, 304, 1487–1490, 2004b.